Letter

Novel One-Dimensional Organometallic Half Metals: Vanadium-Cyclopentadienyl, Vanadium-Cyclopentadienyl-Benzene, and Vanadium-Anthracene Wires

Lu Wang, Zixing Cai, Junyu Wang, Jing Lu, Guangfu Luo, Lin Lai, Jing Zhou, Rui Qin, Zhengxiang Gao, Dapeng Yu, Guangping Li, Wai Ning Mei, and Stefano Sanvito

More About This Article

Additional resources and features associated with this article are available within the HTML version:

- Supporting Information
- Access to high resolution figures
- Links to articles and content related to this article
- Copyright permission to reproduce figures and/or text from this article

View the Full Text HTML

Novel One-Dimensional Organometallic Half Metals: Vanadium-Cyclopentadienyl, Vanadium-Cyclopentadienyl-Benzene, and Vanadium-Anthracene Wires

Lu Wang,[†] Zixing Cai,[†] Junyu Wang,[†] Jing Lu,[†,‡,*] Guangfu Luo,[†] Lin Lai,[†] Jing Zhou,[†] Rui Qin,[†] Zhengxiang Gao,[†,*] Dapeng Yu,[†] Guangping Li,[§] Wai Ning Mei,[‡] and Stefano Sanvito[⊥]

State Key Laboratory for Mesoscopic Physics and Department of Physics, Peking University, Beijing 100871, Peoples Republic of China, Department of Physics, University of Nebraska at Omaha, Omaha, Nebraska 68182-0266, SICAS Center, Lee Hall, SUNY Oneonta, Oneonta, New York 13820, and School of Physics and CRANN, Trinity College, Dublin 2, Ireland

Received June 4, 2008; Revised Manuscript Received August 27, 2008

ABSTRACT

By using the density functional theory, we find that organometallic multidecker sandwich clusters $V_{2n+1}Cp_{2n+2}$, $V_n(FeCp_2)_{n+1}$ (Cp = cyclopentadienyl), and $V_{2n}Ant_{n+1}$ (Ant = anthracene) may have linear structures, and their total magnetic moments generally increase with the cluster size. The one-dimensional $(VCp)_\infty$, $(VBzVCp)_\infty$ (Bz = benzene), and $(V_2Ant)_\infty$ wires are predicted to be ferromagnetic half-metals, while the one-dimensional $(VCpFeCp)_\infty$ wire is a ferromagnetic semiconductor. The spin transportation calculations show that the finite $V_{2n+1}Cp_{2n+2}$ and $V_n(FeCp_2)_{n+1}$ sandwich clusters coupled to gold electrodes are nearly perfect spin-filters.

Spintronics has attracted much interest during the past few years as it holds promise for the next generation of electronic devices with improved performance and enhanced functionality.[1,2] Organic spintronics is an important branch of spintronics, where the spin-polarized signal can be mediated and controlled by organic molecules.[3,4] Organic materials have two significant advantages over inorganic ones when they are used as spintronic devices. First, the spin−orbit and hyperfine interactions are weak in organic molecules,[5,6] leading to considerably long spin relaxation length[7] and spin-lifetime.[8] Second, organic materials are cheap, low-weight, mechanically flexible, and chemically interactive.[6] Organic half-metal is especially important for organic spintronics because 100% spin polarization transportation is available. Recently, one-dimensional vanadium-benzene wire, which is the limiting case of experimentally synthesized multidecker V_nBz_{n+1} (Bz = benzene) sandwich complex,[9−12] is predicted to be an organic half-metal and attracts much attention.[13−15]

The goal of this letter is to search for organic half-metal from multidecker metallocenes and vanadium-anthracene sandwich complexes. The vanadium−iron-cyclopentadienyl clusters $V_n(FeCp_2)_{n+1}$ (Cp = cyclopentadienyl) were synthesized by reacting V vapor with ferrocene (FeCp_2) in 2000,[16] and the vanadium-anthracene clusters were synthesized by reacting V vapor with anthracene in 1999.[9] The two types of clusters are suggested to have linear multidecker sandwich structures.[9,16] In this letter, we investigate two kinds of multidecker metallocenes $V_{2n+1}Cp_{2n+2}$ and $V_n(FeCp_2)_{n+1}$ and one kind of multidecker vanadium-anthracene sandwich structure $V_{2n}Ant_{n+1}$ (Ant = anthracene) by using the density functional theory (DFT). The $V_{2n+1}Cp_{2n+2}$ clusters probably could be produced by reacting V vapor with vanadocene VCp_2, following the procedure to produce $V_n(FeCp_2)_{n+1}$.

Calculations are based on the spin-unrestricted DFT performed within periodic boundary conditions, norm-conserving pseudopotentials, and the linear combination of atomic numerical orbitals formalism as implemented in SIESTA.[17] The generalized gradient approximation (GGA) of the Perdew−Burke−Ernzerhof (PBE)[18] form is used for the exchange−correlation functional. Optimized basis sets of the double-ξ quality including polarization functions are used with the real-space mesh cutoff 400 Ry. For infinite

* To whom correspondence should be addressed. E-mail: (J.L.) jinglu@pku.edu.cn; (Z.X.G.) zxgao@pku.edu.cn.
† Peking University.
‡ University of Nebraska at Omaha.
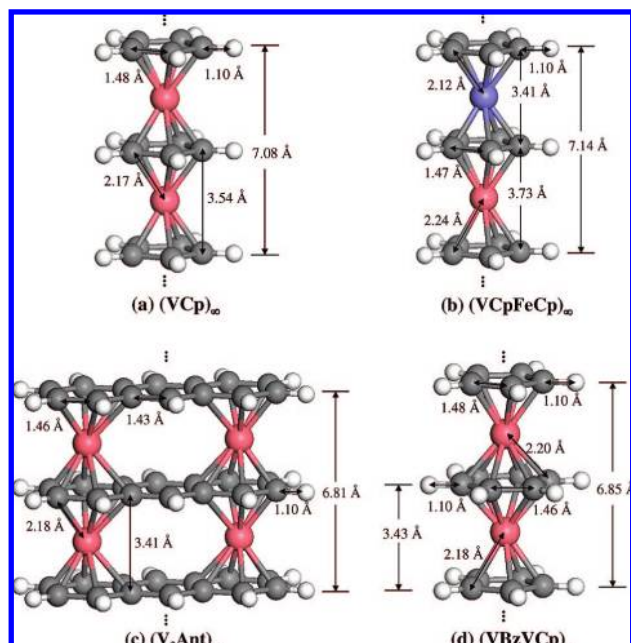§ SUNY Oneonta.
⊥ Trinity College.

Figure 1. Structures of the most stable infinite 1D $(VCp)_\infty$, $(VCpFeCp)_\infty$, $(V_2Ant)_\infty$, and $(VBzVCp)_\infty$ wires. Red ball, V; blue ball, Fe; gray ball, C; white ball, H.

Figure 2. Total magnetic moments of the most stable structures of $V_{2n+1}Cp_{2n+2}$, $V_n(FeCp_2)_{n+1}$, and $V_{2n}Ant_{n+1}$ clusters as a function of the cluster size. Red ball, V; blue ball, Fe; gray ball, C; white ball, H.

1D wires, the Monkhorst−Pack[19] $1 \times 1 \times 50$ k-point grid is used to sample the 1D Brillouin zone.

We consider two types of initial structures for $V_{2n+1}Cp_{2n+2}$ ($n = 1-3$) and $V_n(FeCp_2)_{n+1}$ ($n = 1-3$) clusters and the infinite 1D $(VCp)_\infty$ and $(VCpFeCp)_\infty$ wires: the eclipsed structure with D_{5h} symmetry and the staggered structure with D_{5d} symmetry. Geometry optimization is performed without any symmetry constraint considering different spin-multiplicity states, and no significant structural distortion is observed. Therefore, the growth of free-standing 1D $(VCp)_\infty$ and $(VCpFeCp)_\infty$ wires from the finite multidecker sandwich clusters appears to be mechanically feasible. For a given spin multiplicity state, the total energy differences between the eclipsed and staggered structures are very small (within 0.02 eV per Cp ring), and the rotation of the Cp rings does not cause much difference in the electronic properties. For simplicity, we focus on the eclipsed structure. For $V_{2n}Ant_{n+1}$ ($n = 1-5$) clusters and the infinite 1D $(V_2Ant)_\infty$ wire, only the structures with D_{2h} symmetry (Figure 1c) are investigated, and no significant structural distortion is observed after full geometry optimization. Additional vibrational frequency analysis is performed for the eclipsed V_3Cp_4, V_5Cp_6, $V(FeCp_2)_2$, V_2Ant_2, and V_4Ant_3 clusters by full-electron DFT method with double numerical plus polarization basis set (DNP) as implemented in DMol[3].[20,21] All the examined structures have no imaginary frequency and are local energy minima.

The ground-state total magnetic moments (S) and the average localized magnetic moments of the transition metal (TM) atoms of the multidecker sandwich clusters are listed in Table S1 of the Supporting Information. The localized magnetic moments of the TM atoms are shown in Figure 2. In most of the examined sandwich clusters, high spin states are energetically preferable, suggesting that the TM atoms
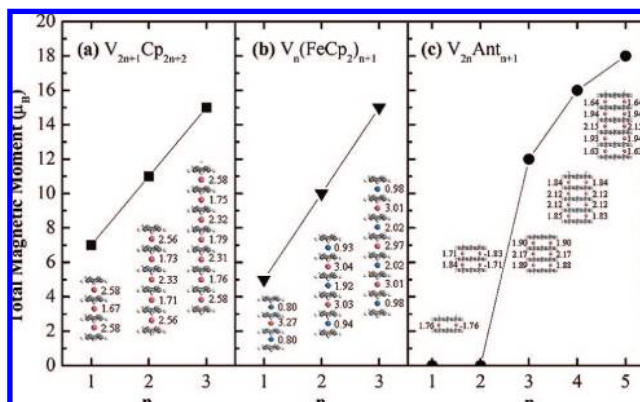
in these clusters are ferromagnetically (FM) ordered in the ground state. The two exceptions are V_2Ant_2 and V_4Ant_3, which have antiferromagnetic (AFM) ground states, and the localized magnetic moments are antiparallel for the two V atoms in the same layer. As shown in Figure 2, S of $V_{2n+1}Cp_{2n+2}$ and $V_n(FeCp_2)_{n+1}$ clusters increases linearly with the cluster size at $n = 1-3$, and S of $V_{2n}Ant_{n+1}$ increases with the cluster size at $n = 3-5$. The linear structure and linear increase of S with the cluster size are also reported for multidecker sandwich V_nBz_{n+1} clusters.[22] The average magnetic moments of the V atom in $V_{2n+1}Cp_{2n+2}$ clusters is about 2.2 μ_B, nearly twice the value in V_nBz_{n+1} clusters, reflecting the less perturbation of the magnetic moment of the V atom by the smaller Cp ring compared with the larger benzene ring.

We define the binding energies (E_b) of multidecker clusters as

$$E_b[V_{2n+1}Cp_{2n+2}] = E[V_{2n+1}Cp_{2n+2}] - nE[V] - (n+1)E[VCp_2] \quad (1)$$

$$E_b[V_n(FeCp_2)_{n+1}] = E[V_nFeCp_2)_n] - nE[V] - (n+1)E[FeCp_2] \quad (2)$$

$$E_b[V_{2n}Ant_{n+1}] = E[V_{2n}Ant_{n+1}] - 2nE[V] - (n+1)E[Ant] \quad (3)$$

The calculated binding energies of the examined multidecker clusters are listed in Table S1 of the Supporting Information with the basis set superposition errors corrected with the fragment relaxation energies.[23] The formation of these multidecker sandwich clusters is always exothermic. The FM states of both the $(VCp)_\infty$ and $(V_2Ant)_\infty$ wires are 0.05 eV per V atoms lower in energy than their AFM states. The FM state of the $(VCpFeCp)_\infty$ wire is 0.36 eV per TM atom lower in energy than its ferrimagnetic (FIM) state. Both the infinite 1D $(VCp)_\infty$ and $(V_2Ant)_\infty$ are half-metallic ferromagnets, whereas the $(VCpFeCp)_\infty$ wire is a ferromagnetic semiconductor. The gaps of the spin minority and majority bands of the three wires are given in Table 1.

We display the spin-polarized band structure and the density of states (DOS) of the infinite 1D $(VCp)_\infty$ wire in

Table 1. Energy Differences between the Antiferromagnetic and Ferromagnetic States Per TM Atom ($E_{AFM} - E_{FM}$), the Band Gap for Majority (Δ_{maj}) and Minority (Δ_{min}) Spin, the Total Magnetic Moment Per Unit Cell (S), the Localized Magnetic Moment on V (S_V), and Fe atoms (S_{Fe}) of the Ground States of the Examined Infinite 1D Wires

	method	$E_{AFM} - E_{FM}$ (eV)	Δ_{maj}	Δ_{min}	S (μ_B)	S_V (μ_B)	S_{Fe} (μ_B)
(VCp)$_\infty$	GGA	0.05	1.0	metallic	2.00	2.05	
	GGA + U	0.33	2.0	metallic			
(VCpFeCp)$_\infty$	GGA	0.36[a]	1.4	1.1	5.00	2.90	2.10
	GGA + U	0.45[a]	1.5	1.5			
(V$_2$Ant)$_\infty$	GGA	0.05	0.8	metallic	4.00	2.00	
	GGA + U	0.11	1.9	metallic			
(VBzVCp)$_\infty$	GGA	0.09	1.1	metallic	3.00	1.64	
	GGA + U	0.26	2.1	metallic			
(VBz)$_\infty$	GGA	0.08[b]	1.18[c]	metallic[c]	0.8[b], 1.00[c]	1.28[c]	
	LDA + U		1.25[c]	metallic[c]			

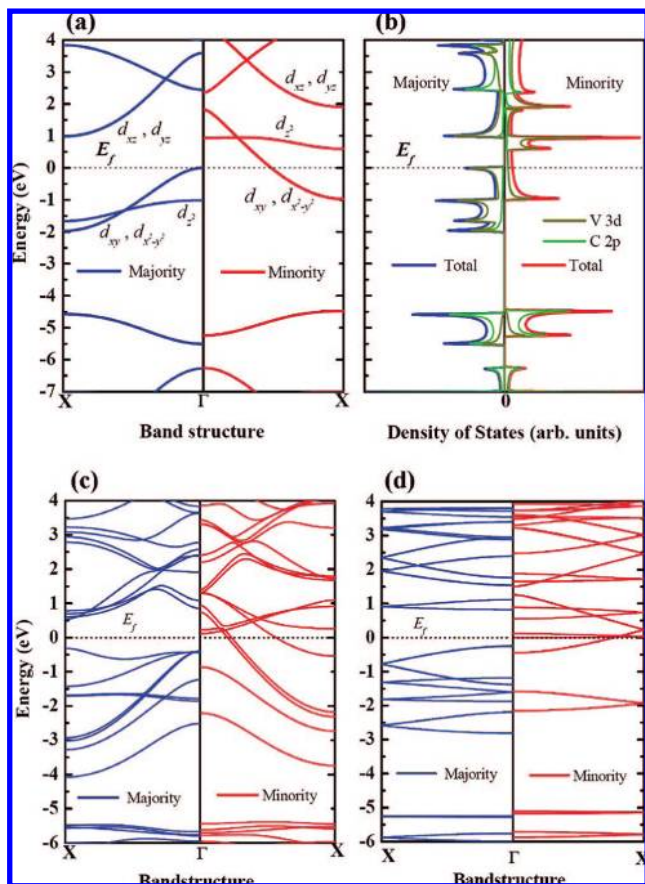[a] $E_{FIM} - E_{FM}$. [b] From ref 13. [c] From ref 14.

Figure 3. Spin-resolved band structures of the infinite 1D (a) (VCp)$_\infty$ (c) (V$_2$Ant)$_\infty$ and (d) (VBzVCp)$_\infty$ wires in their ground state. The spin-resolved total and local density of states of the infinite 1D (VCp)$_\infty$ wire in the ground-state is shown in panel (b), and a strong hybridization occurs between the p orbitals of the Cp ring and the d orbitals of the V atom from the this panel.

Figure 3a,b, respectively. The majority spin of the 1D (VCp)$_\infty$ wire has a semiconducting nature with an indirect band gap of 1.0 eV, whereas the minority spin is metallic, with a doubly degenerate band crossing the Fermi level (E_f). In other words, there are two ballistic conductance channels for the minority spin and none for the majority spin. The bands near E_f are mainly derived from the 3d orbitals of the V atom and the 2p orbitals of the C atom. The strong crystalline field with D_{5h} symmetry splits the 3d levels of V atom into a singlet d_{z^2} orbital and two doublets of d_{xy} and $d_{x^2-y^2}$ orbitals and d_{xz} and d_{yz} orbitals. The d_{xz} and d_{yz}-dominated bands are

pushed above E_f. In the majority spin part, the d_{z^2}, d_{xy} and $d_{x^2-y^2}$-dominated bands are fully occupied. In the minority spin part, the d_{z^2}-dominated band is unoccupied, and the d_{xy} and $d_{x^2-y^2}$-dominated bands are occupied by a mere one electron. Therefore, the total magnetic moment is 2.0 μ_B per unit cell. The localized magnetic moment of the V atom is 2.05 μ_B, significantly larger than that of the V atom (1.28 μ_B) in the (VBz)$_\infty$ (Bz = benzene) wire.[14] On the other hand, the localized magnetic moment distributed over the Cp ring ($-0.05 \mu_B$) in the (VCp)$_\infty$ wire is smaller than that distributed over the benzene ring ($-0.28 \mu_B$) in the (VBz)$_\infty$ wire.[14] We display the spin-polarized band structure of the infinite 1D (V$_2$Ant)$_\infty$ in Figure 3c. The majority spin has a direct band gap of 0.8 eV at X-point, and the minority spin has three ballistic conductance channels. The localized magnetic moment for the V atom is 2.0 μ_B, and the localized magnetic moment distributed over anthracene is negligible. The spin-polarized band structure of the 1D (VCpFeCp)$_\infty$ is provided in the Supporting Information.

The DFT-GGA calculations are known to underestimate the on-site correlation effects between 3d electrons of TM atoms, which are very important for the prediction of the magnetic interaction. Next we have performed calculations within the GGA + U scheme[17] by using the projector augmented wave method[18] as implemented in VASP.[19] The parameter $U - J$ is set to 3 and 2 eV for the V and Fe atoms, respectively. The main results of the two methods are compared in Table 1. The half-metal identification for the 1D (VCp)$_\infty$ and (V$_2$Ant)$_\infty$ and ferromagnetic semiconductor identification for the 1D (VCpFeCp)$_\infty$ remain valid. The inclusion of a Hubbard U term causes an increase of the energy difference between the FM and AFM/FIM states, and it also causes an increase of the gap of the spin majority band due to a downshift of the d_{z^2}, d_{xy}, and $d_{x^2-y^2}$-dominated bands in the majority spin part.

There are two exchange interactions between the localized magnetic moments of the V atoms: the direct exchange and the indirect superexchange through the π-type orbitals of the Cp ring. We study the magnetic coupling of an isolated V atom chain by removing the Cp ring of the (VCp)$_\infty$ wire and find that the AFM phase is 0.05 and 0.23 eV more stable than the FM phase at the GGA and GGA + U level, respectively. Therefore, the indirect superexchange favors the FM phase and dominates the direct coupling in the

(VCp)∞ wire if the direct exchange is the same in the (VCp)∞ wire and in the isolated V atom chain. The common half-metal feature of the 1D (VCp)∞ and (VBz)∞ wire suggests that novel half-metal sandwich wire may be obtained by partial substitution of the Cp rings by the benzene rings. One possible structure is the 1D (VBzVCp)∞ wire, which has alternate benzene and cyclopentadienyl decks. Experimentally, triple-decker sandwich CpVBzVCp cluster has been synthesized.[24] The FM phase for the 1D (VBzVCp)∞ wire is 0.09 and 0.26 eV per V atoms lower in energy than its AFM phase at the GGA and GGA + U level, respectively, and this FM phase is indeed a half-metallic ferromagnet at both levels.

The key electronic properties of the 1D (VBzVCp)∞ wire are given in Table 1. The rotation of the Cp and Bz rings does not cause much difference in the electronic or magnetic properties. We display the spin-polarized band structure of the infinite 1D (VBzVCp)∞ wire in Figure 3d. The majority spin has a direct bandgap of 1.1 and 2.1 eV at X-point at the GGA and GGA + U level, respectively, and the minority spin has one ballistic conductance channel. The localized magnetic moment for the V atom is 1.64 μ_B, and the localized magnetic moments distributed over the Cp and benzene rings are −0.06 and −0.22 μ_B, respectively. We have optimized finite multidecker sandwich V_2BzCp_2, $V_4Bz_2Cp_3$, and $V_6Bz_3Cp_4$ clusters without any symmetry constraint considering different spin-multiplicity states and found they have linear structures and high spin ground states, and the total magnetic moment of the ground-state also increases with the cluster size, as shown in Table S1 of the Supporting Information.

Finally, we performed transport calculations for the finite multidecker sandwich clusters based on the DFT and nonequilbrium Green's function method with the code SMEAGOL.[25,26] Two selected clusters V_3Cp_4 and $V(FeCp_2)_2$ are coupled to nonmagnetic metal electrodes (Au (111)), and the Au−V_3Cp_4−Au and Au−$V(FeCp_2)_2$−Au structures have been optimized. The transmission spectra $T(E)$ around E_F are presented in Figure 4. The spin polarization of the electron current is defined as $|T_{min}(E_F) − T_{maj}(E_F)|/[T_{min}(E_F) + T_{maj}(E_F)]$, where T_{min} and T_{maj} represent the transmission coefficient of the minority and majority spin channel, respectively. The calculated spin polarizations of the electron current are 95% for V_3Cp_4 and 92% for $V(FeCp_2)_2$, suggestive of highly effective spin-filters. As shown in Table S1 of the Supporting Information, the highest occupied molecular orbital (HOMO)−lowest unoccupied molecular orbital (LUMO) gap of the V_3Cp_4 cluster for the majority spin channel (1.6 eV) is somewhat larger than that (1.1 eV) for the minority spin channel, and the HOMO−LUMO gap of $V(FeCp_2)_2$ for the minority spin channel (2.7 eV) is much larger than that (0.4 eV) for the majority spin channel. These differences in the HOMO−LUMO gap between different spins account for the spin polarization of the electron current in both V_3Cp_4 and $V(FeCp_2)_2$. However, the comparable spin polarization of V_3Cp_4 and $V(FeCp_2)_2$, though the HOMO−LUMO gap difference between the two spin channels in V_3Cp_4 is much smaller than that in $V(FeCp_2)_2$, implies that the finite
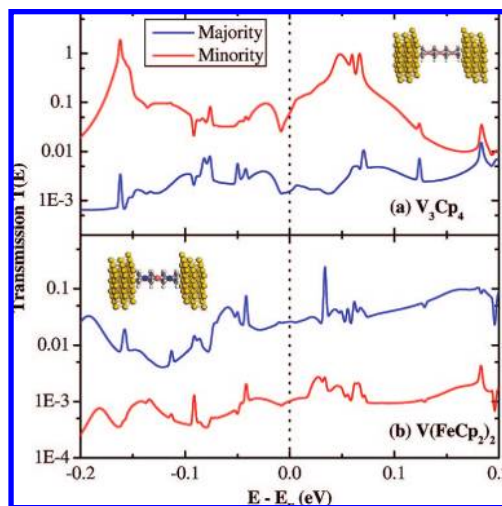

Figure 4. Transmission spectra of the (a) V_3Cp_4 and (b) $V(FeCp_2)_2$ clusters coupled to gold electrodes. Inset: the corresponding structures.

cluster of a half-metal wire is more effective as a spin filter than that of a non half-metal FM wire.

In conclusion, we reveal that the organometallic multidecker sandwich complexes $V_{2n+1}Cp_{2n+2}$, $V_n(FeCp2)_{n+1}$, and $V_{2n}Ant_{n+1}$ are linear ferromagnetic clusters up to n = 3, 3, and 5, respectively, except V_2Ant_2 and V_4Ant_3. The infinite 1D (VCp)∞, (VBzVCp)∞, and $(V_2Ant)_∞$ wires turn out to be half-metallic ferromagnets, whereas the (VCpFeCp)∞ wire is a ferromagnetic semiconductor. The $V_{2n+1}Cp_{2n+2}$ and $V_n(FeCp2)_{n+1}$ clusters coupled to gold electrodes could be used to generate spin-polarized currents and serve as highly effective spin-filters.

After completion of this manuscript, we became aware of a recent job of Zhou et al.[27] who proposed that the 1D iron-cyclopentadienyl sandwich wire (FeCp)∞ is a half-metal from DFT calculations. Our calculation also confirms that the 1D (FeCp)∞ wire is indeed a half-metal. However, the structural stability of the finite linear multidecker Fe_nCp_m clusters was not checked therein, and the growth of the 1D (FeCp)∞ wire from the finite multidecker sandwich cluster is infeasible if the finite multidecker Fe_nCp_m clusters undergo a significant structural deviation from a linear structure.

Supporting Information Available: Binding energies, HOMO−LUMO gaps, and magnetic moments of the most stable structures of $V_{2n+1}Cp_{2n+2}$, $V_n(FeCp_2)_{n+1}$, $V_{2n}Ant_{n+1}$, and $V_{2n}Bz_nCp_{n+1}$ multidecker clusters, and the spin-resolved electronic band structure of the 1D (VCpFeCp)∞ wire. This

material is available free of charge via the Internet at http://pubs.acs.org.

References

(1) Wolf, S. A.; Awschalom, D. D.; Buhrman, R. A.; Daughton, J. M.; von Molnar, S.; Roukes, M. L.; Chtchelkanova, A. Y.; Treger, D. M. *Science* **2001**, *294*, 1488.

(2) Zutic, I.; Fabian, J.; Das Sarma, S. *Rev. Mod. Phys.* **2004**, *76*, 323.

(3) Naber, W. J. M.; Faez, S.; van der Wiel, W. G. *J. Phys. D: Appl. Phys.* **2007**, *40*, R205.

(4) Xiong, Z. H.; Wu, D.; Vardeny, Z. V.; Shi, J. *Nature* **2004**, *427*, 821.

(5) Sanvito, S. *J. Mater. Chem.* **2007**, *17*, 4455.

(6) Sanvito, S.; Rocha, A. R. *J. Comput. Theor. Nanosci.* **2006**, *3*, 624.

(7) Tsukagoshi, K.; Alphenaar, B. W.; Ago, H. *Nature* **1999**, *401*, 572.

(8) Kikkawa, J. M.; Awschalom, D. D. *Nature* **1999**, *397*, 139.

(9) Kurikawa, T.; Takeda, H.; Hirano, M.; Judai, K.; Arita, T.; Nagao, S.; Nakajima, A.; Kaya, K. *Organometallics* **1999**, *18*, 1430.

(10) Miyajima, K.; Muraoka, K.; Hashimoto, M.; Yasuike, T.; Yabushita, S.; Nakajima, A.; Kaya, K. *J. Phys. Chem. A* **2002**, *106*, 10777.

(11) Miyajima, K.; Nakajima, A.; Yabushita, S.; Knickelbein, M. B.; Kaya, K. *J. Am. Chem. Soc.* **2004**, *126*, 13202.

(12) Miyajima, K.; Yabushita, S.; Knickelbein, M. B.; Nakajima, A. *J. Am. Chem. Soc.* **2007**, *129*, 8473.

(13) Xiang, H. J.; Yang, J. L.; Hou, J. G.; Zhu, Q. S. *J. Am. Chem. Soc.* **2006**, *128*, 2310.

(14) Maslyuk, V. V.; Bagrets, A.; Meded, V.; Arnold, A.; Evers, F.; Brandbyge, M.; Bredow, T.; Mertig, I. *Phys. Rev. Lett.* **2006**, *97*, 097201.

(15) Koleini, M.; Paulsson, M.; Brandbyge, M. *Phys. Rev. Lett.* **2007**, *98*, 197202.

(16) Nagao, S.; Kato, A.; Nakajima, A.; Kaya, K. *J. Am. Chem. Soc.* **2000**, *122*, 4221.

(17) Soler, J. M.; Artacho, E.; Gale, J. D.; Garcia, A.; Junquera, J.; Ordejon, P.; Sanchez-Portal, D. *J. Phys.: Condens. Matter* **2002**, *14*, 2745.

(18) Perdew, J. P.; Burke, K.; Ernzerhof, M. *Phys. Rev. Lett.* **1996**, *77*, 3865.

(19) Monkhorst, H. J.; Pack, J. D. *Phys. Rev. B* **1976**, *13*, 5188.

(20) Delley, B. *J. Chem. Phys.* **1990**, *92*, 508.

(21) Delley, B. *J. Chem. Phys.* **2000**, *113*, 7756.

(22) Wang, J. L.; Acioli, P. H.; Jellinek, J. *J. Am. Chem. Soc.* **2005**, *127*, 2812.

(23) Xantheas, S. S. *J. Chem. Phys.* **1996**, *104*, 8821.

(24) Duff, A. W.; Jonas, K.; Goddard, R.; Kraus, H. J.; Krueger, C. *J. Am. Chem. Soc.* **1983**, *105*, 5479.

(25) Rocha, A. R.; Garcia-Suarez, V. M.; Bailey, S. W.; Lambert, C. J.; Ferrer, J.; Sanvito, S. *Nat. Mater.* **2005**, *4*, 335.

(26) Rocha, A. R.; Garcia-Suarez, V. M.; Bailey, S.; Lambert, C.; Ferrer, J.; Sanvito, S. *Phys. Rev. B* **2006**, *73*, 085414.

(27) Zhou, L. P.; Yang, S.-W.; Ng, M.-F.; Sullivan, M. B.; Tan, V. B. C.; Shen, L. *J. Am. Chem. Soc.* **2008**, *130*, 4023.